

Ribozyme minigene-mediated RAD51 down-regulation increases radiosensitivity of human prostate cancer cells

S. J. Collis^{1,2}, A. Tighe^{1,2}, S. D. Scott^{1,2}, S. A. Roberts², J. H. Hendry² and G. P. Margison^{1,*}

¹Carcinogenesis Group and ²Experimental Radiation Oncology Group, Cancer Research Campaign, Paterson Institute for Cancer Research, Wilmslow Road, Manchester M20 4BX, UK

Received December 4, 2000; Revised and Accepted February 15, 2001

ABSTRACT

The strand transferase RAD51 is a component of the homologous recombination repair pathway. To examine the contribution of RAD51 to the genotoxic effects of ionising radiation, we have used a novel ribozyme strategy. A reporter gene vector was constructed so that expression of an inserted synthetic double-stranded ribozyme-encoding oligonucleotide would be under the control of the cytomegalovirus immediate-early gene enhancer/promoter system. The prostate tumour cell line LNCaP was transfected with this vector or a control vector, and a neomycin resistance gene on the vector was used to create geneticin-resistant stable cell lines. Three stable cell lines were shown by western blot analysis to have significant down-regulation of RAD51 to 20–50% of the levels expressed in control cell lines. All three cell lines had a similar increased sensitivity to γ -irradiation by 70 and 40%, respectively, compared to normal and empty vector-transfected cells, corresponding to dose-modifying factors of ~2.0 and 1.5 in the mid-range of the dose-response curves. The amount of RAD51 protein in transfected cell lines was shown to strongly correlate with the α parameter obtained from fitted survival curves. These results highlight the importance of RAD51 in cellular responses to radiation and are the first to indicate the potential use of RAD51-targeted ribozyme minigenes in tumour radiosensitisation.

INTRODUCTION

It is well known that ionising radiation interacts with cells in a number of ways leading to DNA damage, chromosomal abnormalities, cell cycle arrest and apoptosis with DNA double-strand breaks (DSB) being considered to be the most important type of damage involved in cell killing (1). Mammalian cells have developed two distinct pathways to repair this type of damage, the homologous recombinational repair (HRR) and non-homologous end-joining pathways. A key component of

the HRR pathway is the protein RAD51, which is part of the RAD52 epistasis group that contains numerous related proteins involved in mitotic recombination (2). The RAD51 protein is a major component of HRR at the S/G₂ phase of the cell cycle (3–5), and levels of RAD51 protein are elevated during cell cycle progression to a maximum at G₂ (6).

Many studies have shown the potential use of ribozymes (catalytic RNA species with site-specific cleavage activity) as anti-cancer agents (7–10). As part of our efforts to devise strategies for enhancing the effectiveness of radiation therapy, we have explored the use of ribozyme technology as a means of attenuating RAD51 expression in tumour cells in a gene therapy context. We produced a dual expression vector encoding enhanced green fluorescent protein (EGFP) and a RAD51 mRNA-targeted ribozyme. Transfection of this vector into cultured cells allowed the rapid assessment of the biological effectiveness of the ribozyme by establishing the extent to which expression leads to attenuation of protein expression and increased cell killing following radiation.

MATERIALS AND METHODS

Construction of ribozyme expression vector pREV

The plasmid vector is based on the mammalian expression vector pCGFP (11). The cytomegalovirus immediate early (CMV IE) gene promoter/enhancer, multiple cloning site and SV40 poly(A) elements from the plasmid vector pCI (Promega) were isolated using a *Bam*HI/*Bgl*II double digestion reaction and ligated into a unique *Bam*HI site of pCGFP. Restriction endonuclease digestions and PCR analyses were carried out to confirm the orientation of the insert. This vector was given the name pREV (ribozyme expression vector, see Fig. 1). The activity of both CMV promoters within the pREV construct was determined by inserting the gene for enhanced yellow fluorescent protein (EYFP) into the second CMV-driven cloning site of pREV. The EYFP gene was isolated from the plasmid pEYFP (Clontech) via *Xba*I digestion and then ligated into the ribozyme-encoding oligonucleotide (REO) insertion site of pREV. A control plasmid for CMV-driven EYFP expression (for FACS analysis) was constructed by inserting the EYFP gene into the pC*Neo* plasmid (Promega) to produce pCYFP. Expression of both EGFP and EYFP was compared using FACS analysis of transfected cells (Fig. 2).

*To whom correspondence should be addressed. Tel: +44 161 446 3183; Fax: +44 161 446 3109; Email: gmargison@picr.man.ac.uk
Present addresses:

A.Tighe, School of Biological Sciences, University of Manchester, 2.205 Stopford Building, Oxford Road, Manchester M13 9PT, UK

S.D.Scott, Experimental Oncology Group, Gray Laboratory Cancer Research Trust, Mount Vernon Hospital, Northwood, Middlesex HA6 2JR, UK

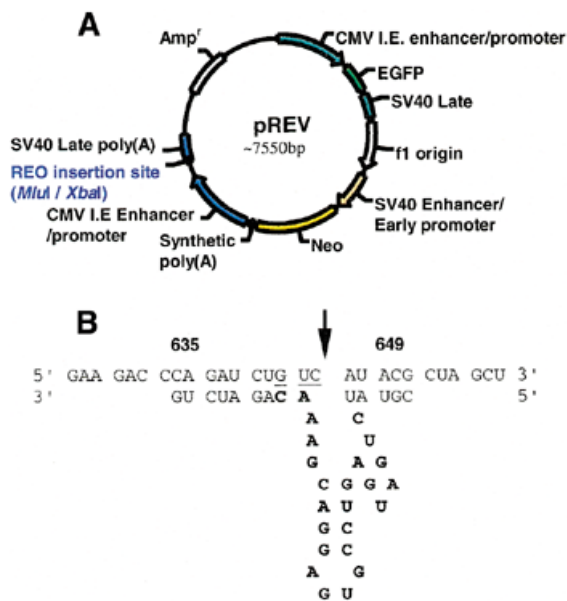


Figure 1. Vector map of pREV and anti-RAD51 ribozyme/target mRNA sequences. (A) The plasmid vector pREV used to insert REOs for expression of ribozymes in mammalian cells. When the RAD51 ribozyme was inserted into pREV, the vector was denoted pREVRz. The gene for EYFP was ligated into the REO insertion site of pREV (called pREYV). (B) RAD51 ribozyme bound to its target mRNA sequence. The top row of nucleotides shows the target molecule with the GUC target site underlined. Bold numbers show residue numbering of the mRNA sequence. The ribozyme is shown underneath and bold letters represent the catalytic core region (16). The arrow indicates the site of cleavage.

REO synthesis and insertion into pREV

A ribozyme was designed to target base pairs 635–649 of the RAD51 mRNA sequence, with cleavage targeted 3' to the 644 cytosine residue (Fig. 1). The corresponding REO was derived from complementary single-stranded oligonucleotides: 5'-CGCGCGTATCTGATGAGTCCGTGAGGACGAAACAGATCTG-3' and 5'-CTAGCAGATCTGTTTCGTCTCACGGACTCATCAGATACG-3', which hybridise to give *Mlu*I- and *Xba*I-compatible overhangs. Double-stranded molecules were produced by mixing 0.05 nmol of each single-stranded oligonucleotide in 5 μ l double-distilled water, heating to 55°C for 5 min, then cooling to room temperature. Mixtures were then incubated with 10 nmol of pREV (digested with *Mlu*I and *Xba*I), in the presence of DNA ligase, overnight at room temperature. The entire ligation reaction was used to transform competent *Escherichia coli* XL1B strain and subsequent ampicillin-resistant clones were screened for insertion of a single REO using colony PCR. One positive clone was chosen and DNA was isolated using a Qiagen maxi-prep kit. The DNA was sequenced using the ABI big dye-terminator kit to confirm integrity of the RAD51 REO. The RAD51 REO-pREV construct was denoted pREVRz.

Cell culture

The human prostate cancer cell line LNCaP was obtained from the American Type Culture Collection. Cells were maintained as adherent monolayer cultures in RPMI-1640 culture medium (Gibco BRL), supplemented with 10% foetal calf serum (FCS;

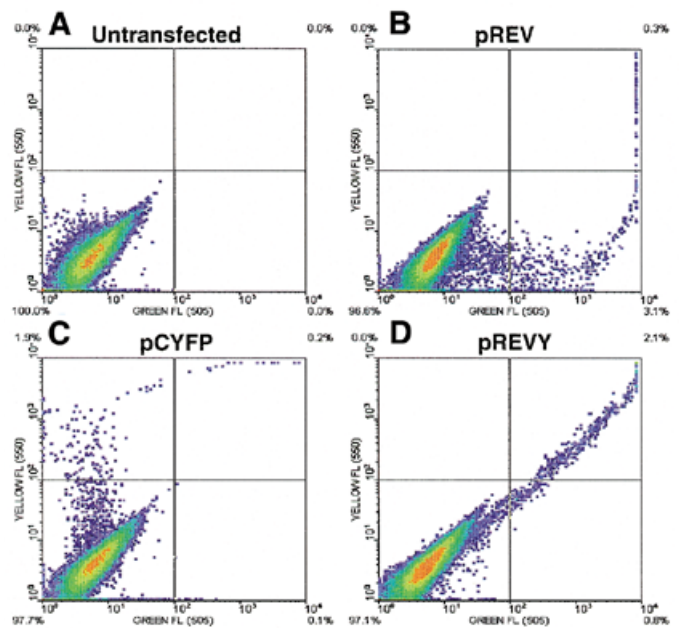


Figure 2. FACS analyses of LNCaP cells 24 h post-transfection with various fluorescent protein-expressing vectors. Cells were transfected with 5 μ g of DNA. (A) Untransfected cells; (B–D) cells transfected with pREV, pCYFP and the pREYV vector, respectively. The angle of yellow/green fluorescence slope (D) shows that both EGFP and EYFP are expressed at very similar levels within cells transfected with the pREYV vector.

Biological Industries), 1 mM L-glutamine, 100 IU/ml penicillin and 0.1 mg/ml streptomycin (all obtained from Gibco BRL). Cells were grown at 37°C in a humidified atmosphere of 5% carbon dioxide, fed every 5 days with complete medium and sub-cultured when confluence was reached.

Transfection of cells/creation of stable cell lines

A total of 2×10^5 cells were seeded into each well of a 6-well tissue culture plate (Falcon). The following day (when the cells were 70–80% confluent) the culture medium was aspirated and the cell monolayer was washed with pre-warmed sterile phosphate-buffered saline. Cells were transfected using Escort™ reagent (Sigma) according to the manufacturer's protocol. Green/yellow fluorescence was analysed 24 h later by FACS (see below). FACS analyses routinely indicated that 20–30% of a transfected population takes up the plasmid and expresses green/yellow fluorescence. The following day, cells were trypsinised to form a single cell suspension. For stable cell lines, they were counted and 2×10^5 cells resuspended in 10 ml of RPMI-160 (10% FCS) supplemented with 0.5 mg/ml geneticin (Gibco BRL) and were plated into separate 10 cm culture dishes. The medium was changed every 5 days. After 2 weeks all untransfected cells had died, and pREV- and pREVRz-transfected cells had formed individual colonies. Two weeks later, colonies from each plate were picked and seeded into separate wells in a 24-well plate (Falcon). Each cell line was then expanded and cell extracts were prepared for western analyses to ascertain cellular levels of RAD51.

FACS analysis

FACS analysis was carried out on transfected cells as previously described (11). Dual-colour FACS was performed as described by Lybarger *et al.* (12), with the addition of a 480 ± 25 nm bandpass filter, which was added to overcome compensation difficulties and allow EGFP emission to be collected at 505 nm. Fluorescence was plotted as density plots using WinMidi 2.8 with EGFP and EYFP expression plotted on the *x*- and *y*-axes, respectively (a 4-log scale was used for each axis).

Western blot analysis

Standard western blot procedures were used. A total of 10 μ g of protein extracted from each cell line was used per blot. An anti-RAD51 antibody (Oncogene) was used for all blots, which were then re-probed with an anti-actin antibody (Sigma). RAD51 levels of three separate blots were normalised to actin levels and quantified using the Scion Image analysis program. A two-tailed *t*-test was used to calculate the level of significance of normalised RAD51 levels between cell lines.

Growth inhibition assays

The MTT growth inhibition assay was carried out as described by Marples *et al.* (11). Plates were irradiated (24 h post-seeding) at 37°C using a ^{60}Co γ -ray source (1.12 Gy/min) and immediately replaced in the incubator for 5 days. Growth inhibition, used as a measure of cytotoxicity, was calculated for each cell line as a percentage growth of the irradiated to unirradiated mean values. These data were then plotted and a linear quadratic function was used to fit dose/growth inhibition curves to the data points. Statistical analysis was carried out using a non-linear regression model of the form $\text{OD} = A\exp(-\alpha D - \beta D^2)$. Separate control growth parameters (*A*) were fitted for each cell line, and common α and β parameters were fitted for different experiments with cell lines of the same individual type, i.e. LNCaP, empty vector- or ribozyme-transfected cells. Variance ratio *F*-tests were used to compare models and to test for parameter value differences between groups.

RESULTS

Rationale

The aim of the present study was to target RAD51 on the HRR pathway of DSB repair to assess if this would affect cellular radiation sensitivity. The strategy used was to express a minigene encoding a ribozyme designed to cleave the RAD51 mRNA. The initial intention was to use a dual expression vector that would express both the ribozyme minigene and the reporter protein, EGFP, so that the effect of ribozyme expression could be monitored in cells taking up and expressing the vector, as indicated by EGFP expression. Figure 1 shows the structure of the plasmid, the sequence of the ribozyme moiety expressed and its target sequence in the RAD51 mRNA.

Both CMV promoters in pREV are equally effective

To confirm that the two CMV promoters within pREV were active, two different fluorescent markers were used to ascertain the activities of the CMV promoters within pREV (see Materials and Methods). The cell line LNCaP was transfected with pREVV (encoding both EGFP and EYFP) and FACS analysis

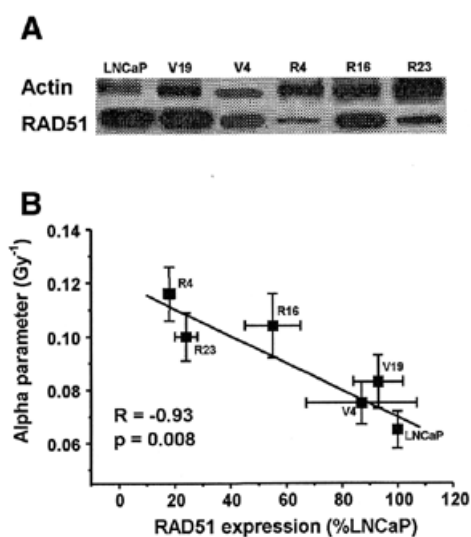


Figure 3. RAD51 expression in normal LNCaP, pREV- and pREVRz-transfected cells. V represents the pREV transfected cell lines, while R represents cell lines derived from cells transfected with the pREVRz construct. (A) A typical western blot, probing for both RAD51 and actin. A total of 10 μ g of protein was loaded in each lane. (B) Correlations between the mean normalised RAD51 levels derived from three independent western blots (two blots for V4) and the α parameter obtained from fitted survival curves for each cell line (see Table 1 and Fig. 4). The corresponding correlation coefficient and *P* value are shown on the graph. A similar correlation was seen when RAD51 expression was compared with the fractional growth at 2 Gy ($R = 0.83$, $P = 0.042$).

was carried out 24 h post-transfection. A control for each fluorescent protein was included in the experiment; pREV was used to show normal expression levels of EGFP, and pCYFP was used for EYFP expression. It was demonstrated that the two promoters showed almost equal activity within pREVV (Fig. 2) and therefore would likely exhibit similar activities in pREV. This alleviated any concerns about possible attenuated expression of the RAD51 REO inserted into the CMV-driven REO insertion site.

Increased sensitivity to ionising radiation in pREVRz-transfected cell lines

LNCaP cells were transfected with pREV and pREVRz, and geneticin-resistant stable cell lines were selected. Levels of RAD51 in cell extracts from stable cell lines were determined by western blot analysis. Three pREVRz-transfected cell lines (R4, R16 and R23) showed a significant reduction in the amount of cellular RAD51 when compared to normal LNCaP cells and cell lines transfected with pREV (V4 and V19, see Fig. 3A). Three independent blots were used to calculate normalised RAD51 levels (except for V4, where two blots were used). Up to 80% down-regulation of RAD51 expression (compared to normal cells and pREV-transfected cells) was observed in cell lines that had been transfected with pREVRz. There was a trend for a slight decrease in RAD51 levels within the V4 and V19 cell lines, which might have been a consequence of inter-clonal variation in the average levels of expression of RAD51 in the clones selected. Figure 3B shows that the amount of cellular RAD51 in both normal and transfected LNCaP cell lines strongly correlated with the α parameter,

Table 1. Growth fractions at 2 and 8 Gy and fitted curve parameters for the six cell lines

Parameter	Cell line					
	LNCaP	V19	V4	R4	R16	R23
SF ₂	0.900 ± 0.020	0.860 ± 0.030	0.840 ± 0.030	0.790 ± 0.040	0.750 ± 0.030	0.790 ± 0.030
SF ₈	0.730 ± 0.020	0.660 ± 0.010	0.690 ± 0.010	0.500 ± 0.010	0.580 ± 0.010	0.550 ± 0.020
α (Gy ⁻¹)	0.065 ± 0.007	0.083 ± 0.010	0.075 ± 0.008	0.116 ± 0.010	0.104 ± 0.012	0.100 ± 0.009
α-α(LNCaP) (<i>P</i> values)	–	0.013 ± 0.005 (0.012)		0.043 ± 0.006 (<0.001)		
Ratio of α values	–	V/LNCaP 1.22 ± 0.18		R/LNCaP 1.68 ± 0.22		R/V 1.38 ± 0.16

Mean values at each dose are shown in bold with their respective standard errors. Growth fractions were calculated from the linear quadratic fitted curves of MTT growth inhibition assays. Common α parameters were fitted for different experiments with cells of the same type and a common β parameter of -0.0034 (± 0.0007) Gy⁻² was fitted for all curves. Differences in the α parameters are shown with their respective *P* values. The ratio between the α parameter of each cell line versus a control is shown with their respective standard errors and 95% confidence intervals in parentheses (calculated using Fieller's theorem).

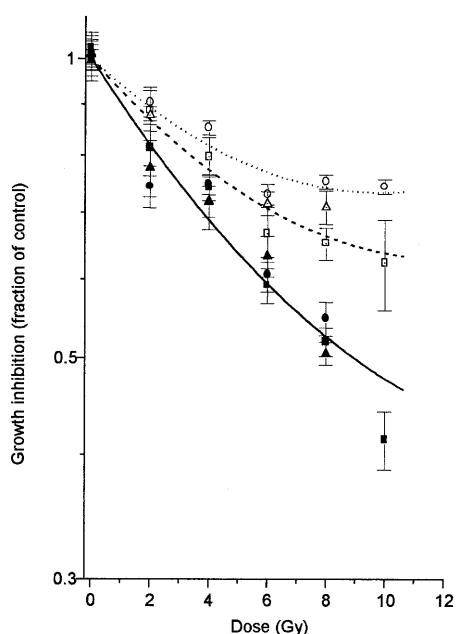


Figure 4. MTT growth inhibition curves. Each point represents 24 measurements; eight repeats per cell line per plate and three plates for each dose. Growth inhibition was calculated as irradiated:unirradiated mean cell growth for each cell line. A linear quadratic fit was used to produce all the curves. Common α and β parameters were fitted for different experiments, with cell lines of the same individual type, i.e. LNCaP, empty vector or ribozyme-transfected cells, and a common β parameter of -0.0034 (± 0.0007) Gy⁻² was fitted for all curves. Open circles, LNCaP; open triangles, V4; open squares, V19; closed squares, R4, closed circles, R16; closed triangles, R23. Fitted functions: dotted line, LNCaP; dashed line, empty vector-transfected cells; solid line, ribozyme-transfected cells.

which quantifies the initial slope of the survival curve, i.e. the sensitivity of the cells at low doses of radiation, and growth fraction at 2 Gy obtained from the fitted survival curves.

Figure 4 shows growth inhibition curves (linear quadratic fit) for these six cell lines following doses of 0–10 Gy. All three pREVRz-transfected cell lines showed an increased radiosensitivity compared to normal LNCaP cells and pREV-transfected controls, with the difference in survival becoming

more apparent after higher doses. The fitted curves were used to estimate dose-modifying factors for the same level of growth inhibition; these were ~ 2.0 and 1.5 for all three pREVRz-transfected cell lines compared to the parental line and the pREV-transfected cell lines, respectively. α parameters were obtained from the fitted curves and compared between the different cell lines to assess differences in radiosensitivity. There was a $68 \pm 22\%$ increase in sensitivity between ribozyme-transfected and parental LNCaP cells, and a $38 \pm 16\%$ increase between ribozyme- and empty vector-transfected cells (Table 1). pREV-transfected cells were slightly ($22 \pm 18\%$) more sensitive to ionising radiation than the parental LNCaP cells, probably a consequence of clonal variation in the mean levels of RAD51 expression (see above). However, the ribozyme-transfected cells were significantly more radiosensitive than both the normal LNCaP cells and the pREV-transfected controls ($P < 0.001$) and this increased radiosensitivity of the three ribozyme-transfected cell lines becomes more evident at higher doses (Table 1). Hence, these results show that stable cell lines derived from LNCaP cells transfected with pREVRz have attenuated expression of RAD51, which results in an increased radiosensitivity.

DISCUSSION

In the present study, a reporter gene expression vector has been engineered to encode a ribozyme specifically targeted towards RAD51 mRNA. Western blot analysis showed that cell lines established from cells transfected with the pREVRz construct had, in some cases, only $\sim 20\%$ RAD51 expression compared to normal cells or those that were transfected with only the pREV construct. The cell line R4, which had the lowest RAD51 levels, exhibited $\sim 50\%$ growth inhibition at 8 Gy compared with $\sim 30\%$ growth inhibition seen in pREV-transfected and parental LNCaP cell lines. The levels of RAD51 protein in transfected cells compared to LNCaP was shown to strongly correlate to the α parameter obtained from fitted growth inhibition curves for each cell line (Fig. 3). Therefore, these results indicate that RAD51 plays an important role in the cellular sensitivity to ionising radiation in this prostate cancer cell line. They also indicate that RAD51

may be a critical factor in the repair of potentially lethal radiation damage in DNA. Whether or not this will apply to other cell types and, more importantly, tumours, remains to be established.

Our results are supported by two recent studies that have highlighted the importance of RAD51 in DNA repair following ionising-radiation-induced damage. Over-expression of RAD51 protein in Chinese hamster ovarian cells conferred an increased radioresistance when the cells were irradiated in late S/G₂ (13). Also, antisense oligonucleotides have been used to down-regulate RAD51 expression, leading to increased radiosensitivity of mouse glioma cell lines after high but not low doses of radiation and an increased survival rate for glioma-bearing mice when treated with the RAD51 antisense molecule prior to irradiation (14,15). Our approach demonstrates that ribozyme minigenes provide an alternative to the use of antisense oligonucleotides.

Current radiotherapy regimes commonly consist of some 30 or more daily 2 Gy exposures, and only a slight radiosensitisation is required at each dose to give a large overall increased cell killing. Theoretically, the radiosensitisation reported here, representing a dose-modifying factor of ~2.0, might be capable of producing high accumulated levels of cell kill.

The potential advantage of the dual reporter gene-ribozyme expression vector is that the effectiveness of the ribozyme can be assessed in transient assays by dual immunofluorescence-immunohistochemical analysis, given appropriate antibodies to the target protein. This was not realised in the present study, but the same vector would allow the very rapid testing of ribozyme minigenes directly in cultured cells in future studies.

ACKNOWLEDGEMENTS

The authors thank Dr Brian Marples and Ms Amanda Watson for advice. This work was supported by the Cancer Research Campaign.

REFERENCES

- Iliakis,G. (1991) The role of DNA double strand breaks in ionising radiation-induced killing of eukaryotic cells. *Bioessays*, **13**, 641–648.
- Thompson,L.H. and Schild,D. (1998) The contribution of homologous recombination in preserving genome integrity in mammalian cells. *Biochimie*, **81**, 87–105.
- Shinohara,A., Ogawa,H. and Ogawa,T. (1992) Rad51 protein involved in repair and recombination in *S. cerevisiae* is a RecA-like protein. *Cell*, **69**, 457–470.
- Benson,F.E., Stasiak,A. and West,S.C. (1994) Purification and characterization of the human Rad51 protein, an analogue of *E. coli* RecA. *EMBO J.*, **13**, 5764–5771.
- Sonoda,E., Sasaki,M.S., Buerstedde,J.M., Bezzubova,O., Shinohara,A., Ogawa,H., Takata,M., Yamaguchi-Iwai,Y. and Takeda,S. (1998) Rad51-deficient vertebrate cells accumulate chromosomal breaks prior to cell death. *EMBO J.*, **17**, 598–608.
- Chen,F., Nastasi,A., Shen,Z., Brenneman,M., Crissman,H. and Chen,D.J. (1997) Cell cycle-dependent protein expression of mammalian homologs of yeast DNA double-strand break repair genes Rad51 and Rad52. *Mutat. Res.*, **384**, 205–211.
- Scanlon,K.J., Ishida,H. and Kashani-Sabet,M. (1994) Ribozyme-mediated reversal of the multidrug-resistant phenotype. *Proc. Natl Acad. Sci. USA*, **91**, 11123–11127.
- Ohta,Y., Kijima,H., Ohkawa,T., Kashani-Sabet,M. and Scanlon,K.J. (1996) Tissue-specific expression of an anti-*ras* ribozyme inhibits proliferation of human malignant melanoma cells. *Nucleic Acids Res.*, **24**, 938–942.
- Dorai,T., Perlman,H., Walsh,K., Shabsigh,A., Goluboff,E.T., Olsson,C.A. and Buttyan,R. (1999) A recombinant defective adenoviral agent expressing anti-bcl-2 ribozyme promotes apoptosis of bcl-2-expressing human prostate cancer cells. *Int. J. Cancer*, **82**, 846–852.
- Welch,P.J., Barber,J.R. and Wong-Staal,F. (1998) Expression of ribozymes in gene transfer systems to modulate target RNA levels. *Curr. Opin. Biotechnol.*, **9**, 486–496.
- Marples,B., Scott,S.D., Hendry,J.H., Embleton,M.J., Lashford,L.S. and Margison,G.P. (2000) Development of synthetic promoters for radiation-mediated gene therapy. *Gene Ther.*, **7**, 511–517.
- Lybarger,L., Dempsey,D., Patterson,G.H., Piston,D.W., Kain,S.R. and Chervenak,R. (1998) Dual-color flow cytometric detection of fluorescent proteins using single-laser (488-nm) excitation. *Cytometry*, **31**, 147–152.
- Vispe,S., Cazaux,C., Lesca,C. and Defais,M. (1998) Overexpression of Rad51 protein stimulates homologous recombination and increases resistance of mammalian cells to ionizing radiation. *Nucleic Acids Res.*, **26**, 2859–2864.
- Taki,T., Ohnishi,T., Yamamoto,A., Hiraga,S., Arita,N., Izumoto,S., Hayakawa,T. and Morita,T. (1996) Antisense inhibition of the RAD51 enhances radiosensitivity. *Biochem. Biophys. Res. Commun.*, **223**, 434–438.
- Ohnishi,T., Taki,T., Hiraga,S., Arita,N. and Morita,T. (1998) *In vitro* and *in vivo* potentiation of radiosensitivity of malignant gliomas by antisense inhibition of the RAD51 gene. *Biochem. Biophys. Res. Commun.*, **245**, 319–324.
- Haseloff,J. and Gerlach,W.L. (1988) Simple RNA enzymes with new and highly specific endoribonuclease activities. *Nature*, **334**, 595–591.